



# Influence of the Wavelength on the Series and Shunt Resistances of a Polycrystalline Silicon Solar Cell n<sup>+</sup>-p-p<sup>+</sup> in Frequency Modulation

Mountaga BOIRO<sup>1#</sup> , Amadou DIAO<sup>1</sup>, Adama NDIAYE<sup>1</sup>, Ibrahima TOURE<sup>1</sup>, Senghane MBODJI<sup>2</sup>

<sup>1</sup>Laboratory of Semiconductors and Solar Energy, Department of Physics, Faculty of Sciences and Techniques, University of Cheikh Anta DIOP, Dakar/Senegal.

<sup>2</sup>Research Team in Renewable Energy, Materials and Laser, Department of Physics, UFRSATIC, University of Alioune DIOP, Bambey, Senegal.

#corresponding author

**Type of Work:** Peer Reviewed.

DOI: <https://dx.doi.org/10.21013/jas.v18.n1.p2>

**Review history:** Submitted: Feb 03, 2023; Revised: March 07, 2023; Accepted: March 11, 2023.

## How to cite this paper:

BOIRO, M., DIAO, A., NDIAYE, A., TOURE, I., MBODJI, S.. (2023). Influence of the Wavelength on the Series and Shunt Resistances of a Polycrystalline Silicon Solar Cell n<sup>+</sup>-p-p<sup>+</sup> in Frequency Modulation. *IRA-International Journal of Applied Sciences* (ISSN 2455-4499), 18(1), 20-31. <https://dx.doi.org/10.21013/jas.v18.n1.p2>

© IRA Academico Research.

 This work is licensed under a [Creative Commons Attribution-NonCommercial 4.0 International License](https://creativecommons.org/licenses/by-nc/4.0/) subject to a proper citation to the publication source of the work.

**Disclaimer:** The scholarly papers as reviewed and published by IRA Academico Research are the views and opinions of their respective authors and are not the views or opinions of IRA Academico Research. IRA Academico Research disclaims any harm or loss caused due to the published content to any party.

IRA Academico Research is an institutional publisher member of *Publishers International Linking Association Inc. (PILA-CrossRef)*, USA. IRA Academico Research is an institutional signatory to the *Budapest Open Access Initiative, Hungary* advocating the open access of scientific and scholarly knowledge. IRA Academico Research is also a registered content provider under *Open Access Initiative Protocol for Metadata Harvesting (OAI-PMH)*.

This paper is peer-reviewed under IRA Academico Research's [Peer Review Program](#).

Mountaga BOIRO /0009-0001-9742-2220

### ABSTRACT

A study of the illumination wavelength effect on the series and shunt resistances of a serial vertical junction silicon solar cell in frequency modulation is done. From the continuity equation of the minority carriers' density, the expressions of the minority carriers' density, the photocurrent density, and the photovoltage, are determined. The curves of the I-V characteristic permit us to deduce the series and shunt resistances which depend on the wavelength and frequency modulation. A few values of series and shunt resistances in short and long wavelengths are determined respectively at the open circuit and the short circuit situation.

**Keywords:** Vertical junction cell, Frequency modulation, Wavelength, Series resistance, Shunt resistance.

### Introduction

Determining the series resistances ( $R_s$ ) and the shunt ( $R_{sh}$ ) is very important, in order to improve the quality of the materials of a solar cell and its conversion yield. These parasitic resistances play a significant role and cannot be ignored. The series resistance is mainly due to the volume resistance of the semiconductor, to the metal contacts and interconnections, to the transport of carriers through the diffusion layer, to the resistances contact between the metal and the electrodes [1-5] while the shunt resistance is related to impurities near the junction to the dangling bonds at the semi-conductors surfaces and to the leakage of the minority carriers' that causes a photocurrent drop in the junction [1-5]. A few pieces of research [2-9] have shed light on the effects of shunt and series resistances on the performance of the solar cell.

They show how parasitic series resistance ( $R_s$ ) and shunt resistance ( $R_{sh}$ ) can affect the performance of solar cells and photovoltaic modules. Other works on series and shunt resistance in static regime [10-12], transient regime [13,14], and frequency modulation [15-17] have been done. The aim of this paper is to study the influence of wavelength on ( $R_s$ ) and ( $R_{sh}$ ) of a serial vertical junction silicon photocell in a fixed frequency.

### Theoretical study

Figure 1 shows a unit of an n+-p-p+ serial vertical junction silicon solar cell [18] under monochromatic illumination:

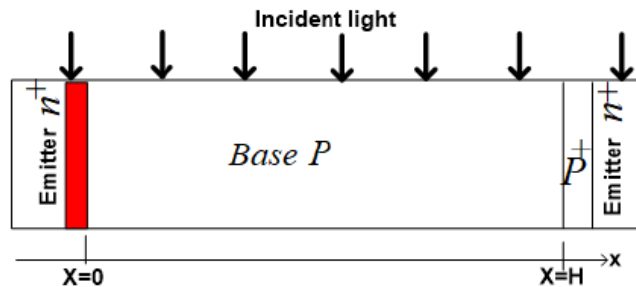


Figure 1. A serial vertical junction solar cell.

This study is based on a vertical junction silicon solar cell, with the following assumptions: the thicknesses of the space charge region and the emitter are very small compared to that of the base; their contributions are then neglected so that only the contribution of the base is considered.

When the solar cell is under an incident light excitation, the phenomena of generation, recombination and diffusion occur in the base. The photogenerated minority carriers in the base, are governed by the following continuity equation in the frequency modulation [19-20].

$$D^* \cdot \frac{\partial^2 \delta(x,z,t)}{\partial x^2} - \frac{\delta(x,z,t)}{\tau} = -G(z,t) + \frac{\partial \delta(x,z,t)}{\partial t} \quad (1)$$

Where  $x$  and  $z$ , represent the depth along the horizontal and that along the vertical, respectively;  $D^*$  [21] is the complex electron scattering diffusion coefficient as a function of modulation frequency;  $\tau$  is the average lifetime of the minority charge carrier and  $t$  is the time.

The overall generation rate is given by [22]:

$$G(z,t) = g(z) \cdot e^{i\omega t} \quad (2)$$

With  $g(z)$  is the spatial component and  $e^{i\omega t}$  the temporal component;  $\omega$  the angular frequency and  $i$  the pure imaginary.

The expression for the generation rate  $g(z)$  is:

$$g(z) = \phi \cdot \alpha \cdot (1 - R) e^{-\alpha z} \quad (3)$$

Where  $\phi$  is the monochromatic incident flux of light;  $\alpha$  the monochromatic absorption coefficient of the material, and  $R$  is the monochromatic reflection coefficient of the material. The minority carriers' density can be put into the form [22, 23]:

$$\delta(x,z,t) = \delta(x,z) \cdot e^{i\omega t} \quad (4)$$

Where  $\delta(x,z)$  is the spatial part.

Substituting equations (2), (3) and (4) into equation (1), we obtain:

$$\frac{\partial^2 \delta(x,z,\lambda,\omega)}{\partial x^2} - \frac{\delta(x,z,\lambda,\omega)}{L^2(\omega)} = -\frac{g(z)}{D(\omega)} \quad (5)$$

We pose:

$$L^2(\omega) = \tau \cdot D(\omega) \quad (6)$$

With  $L(\omega)$  the diffusion length of the minority carriers. The general solution of equation (6) is:

$$\delta(x,z,\lambda,\omega) = K_1 \cdot e^{\frac{x}{L(\omega)}} + K_2 \cdot e^{-\frac{x}{L(\omega)}} + \frac{L^2(\omega)}{D(\omega)} \cdot \phi \cdot \alpha \cdot (1 - R) e^{-\alpha z} \quad (7)$$

The coefficients  $K_1$  and  $K_2$  are determined by the following boundary conditions [24, 25].

- at the Emitter-base junction ( $x = 0$ ):

$$D(\omega) \cdot \frac{\partial \delta(x,z,\lambda,\omega)}{\partial x} \Big|_{x=0} = S_f \cdot \delta(x,z,\lambda,\omega) \Big|_{x=0} \quad (8)$$

- in the middle of the base ( $x = \frac{H}{2}$ ):

$$\frac{\partial \delta(x,z,\lambda,\omega)}{\partial x} \Big|_{x=\frac{H}{2}} = 0 \quad (9)$$

With  $H$  is the thickness of the base of the solar cell along the horizontal;  $S_f$  is the junction recombination velocity [26, 27].

## Result and Discussion

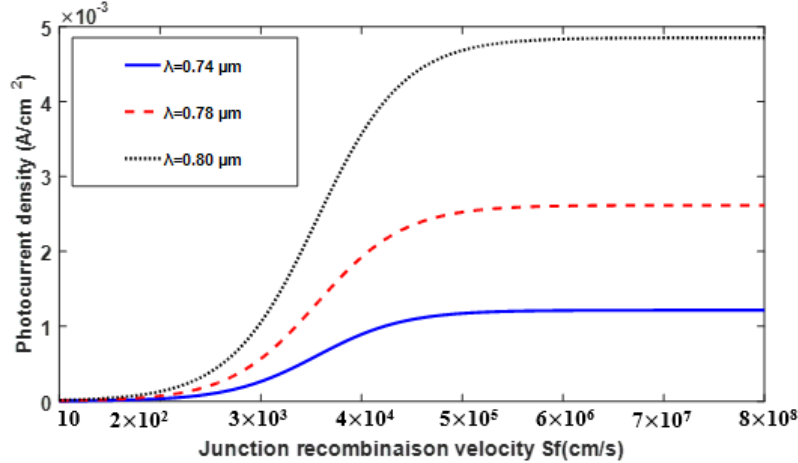
### Photocurrent Density

The excess minority carriers in the base will flow towards the two junctions by diffusion. The obtained photocurrent density is given by [28, 29]:

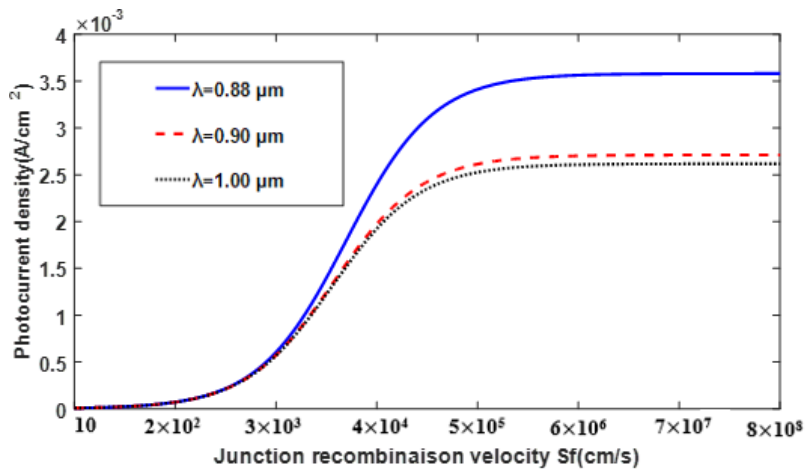
$$J_{ph}(x, z, \lambda, \omega) = q \cdot D(\omega) \left. \frac{\partial \delta(x)}{\partial x} \right|_{x=0} \quad (10)$$

Where  $q$  is the elementary charge

Figures 2-a) and 2-b) show the photocurrent density profile as a function of the recombination velocity at the junction for different wavelengths.



2-a



2-b

Figure 2: The photocurrent density profile as a function of the recombination rate at the junction.  
 2-a: short wavelength, 2-b: long wavelength  
 $\omega_r = 1.75 \times 10^7$ ;  $z = 0.002$  cm

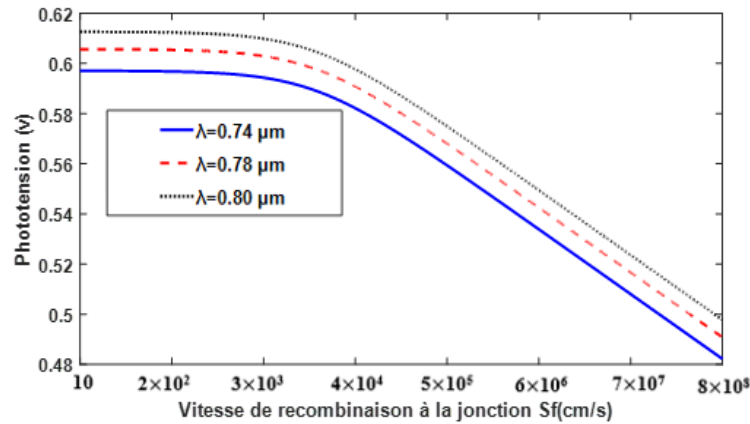
In Figure 2, the photocurrent density is almost zero for low values of the recombination rate at the Sf junction. It increases until it reaches its maximum with the junction recombination velocity Sf. We notice that the photocurrent density increases with the wavelength in the short wavelength range. This is due to the increase in the generation rate (because the short wavelengths generate more carriers in the base of the solar cell). The photocurrent density decreases in the long wavelength range. This decrease is related to the low absorption of the photocell when the incident flux decreases. The effect of the wavelength on the photocurrent density is more sensitive in the short circuit than in the open circuit. The behaviour of the photocurrent density depends on the value of the generation rate which varies according to the different wavelength ranges.

**The Photovoltage**

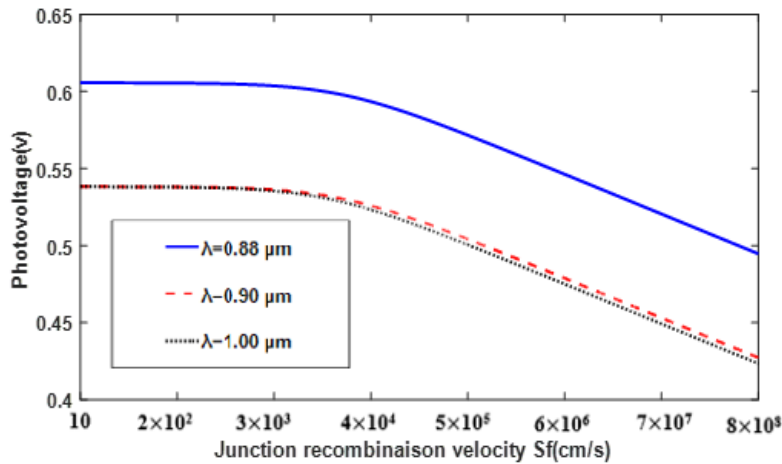
The photovoltaic voltage across the junction, according to the BOLZMANN relation, is obtained as:

$$V_{ph}(x, z, \lambda, \omega) = V_T \cdot \ln \left( 1 + \frac{N_b}{n_i} \cdot \delta(x, z, \lambda, \omega) \Big|_{x=0} \right) \quad (11)$$

Where  $V_T$  the thermal voltage,  $N_b$  the doping rate in the base,  $n_i$  the intrinsic carrier density. Figure 3-a and 3b gives the photovoltage profile as a function of the recombination velocity at the junction for different wavelength:



3-a



3-b

Figure 3: Photovoltage versus recombination rate at the junction.  
 3-a: short wavelength, 3-b: long wavelength  
 $\omega_r = 1.75 \times 10^7$ ;  $z = 0.002 \text{ cm}$

In figures 3-a) and 3-b), the profiles of the photovoltage as a function of the recombination velocity, show the same curves. In figure 3-a), an increase in the wavelength, involves a consequent absorption of the incident photons by the base of the solar cell. This leads to a photogeneration of minority carriers and then a high photovoltage. However, in figure 3-b), the absorption of the base of the incident photons corresponding to the long wavelengths, is weak to the point that the material constituting the solar cell becomes transparent. This implies a photovoltage that decreases since the photogeneration of minority carriers is low.

**The Jph-Vph characteristic**

Figures 4-a and 4b give the profile of the character in the function of the junction recombination velocity for different wavelengths.

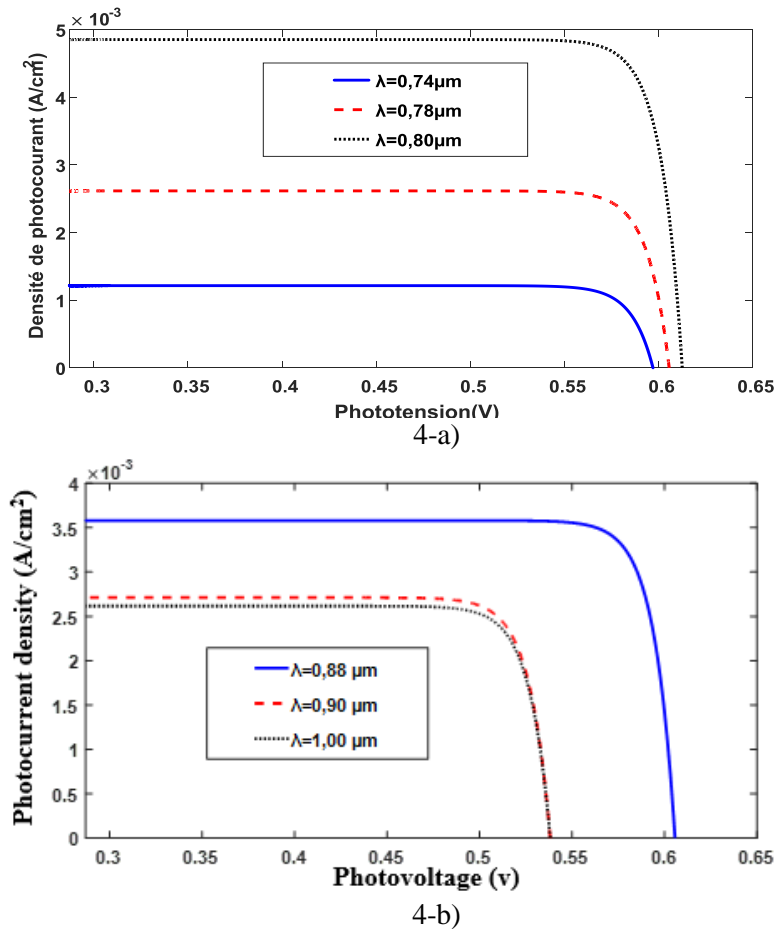


Figure 4: Characteristic Jph-Vph for different values of the wavelength. a) Short wavelength b) Long wavelength  $\omega_r=1.75.10^7$  rad/s;  $z=0.002$  cm

In figure 4, we obtain the same curves of the Jph-Vph characteristics at a well-given applied magnetic field and illumination depth.

In the short wavelength range, that is in figure 4-a), the amplitude of the short circuit photocurrent density and the open circuit photovoltage increases with the wavelength. This corresponds to a high absorption of incident photons by the solar cell followed by an increased photogeneration of minority carriers with enough kinetic energy to cross the junction.

On the other hand, in the interval of long wavelengths, the amplitude of the photocurrent and the open circuit photovoltage, decrease when the wavelength increases. At this level, we note a weak absorption of incident photons by the solar cell; this leads to a weak photogeneration of minority carriers and their probable recombination in volume.

**The Series Resistance (Rs)**

The current-voltage characteristic in the vicinity of the open circuit is an oblique line. Whereas for an ideal voltage generator, this current-voltage characteristic is a vertical line. Since the current-voltage

characteristic above is not a vertical line, we deduce that the solar cell behaves like a real voltage generator. This voltage is comparable to the open circuit photovoltage. As the solar cell is not ideal, it has ohmic losses. These are characterized by the presence in the equivalent circuit of a series resistor ( $R_s$ ), connected in series with the voltage source. The equivalent electrical circuit of the solar cell operating in an open circuit situation is shown in figure [30].

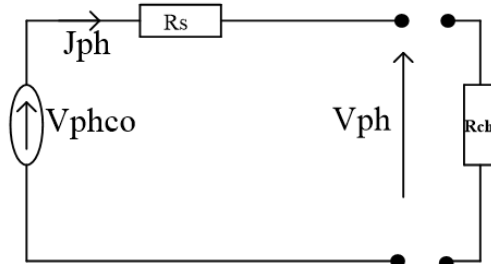


Figure 5: Equivalent electrical circuit of the solar cell operating in an open circuit situation

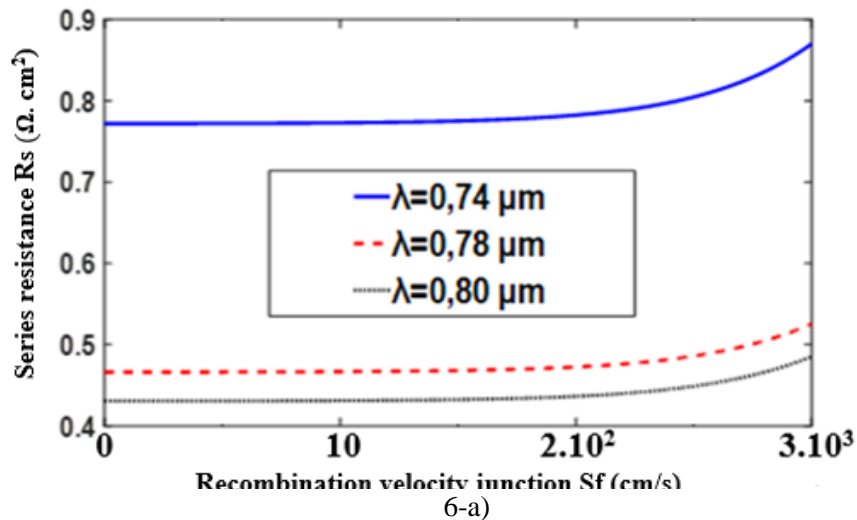
Where  $V_{co}$  is the open circuit photovoltage, and  $R_{ch}$  is the load resistance. By applying the law of meshes we find the series resistance [31, 32]:

$$V_{ph}(\omega, \lambda, z, S_f) = V_{phco}(\omega, \lambda, z) - R_s(\omega, \lambda, z, S_f) \times J_{ph}(\omega, \lambda, z, S_f) \quad (12)$$

So we have:

$$R_s(\omega, \lambda, z, S_f) = \frac{V_{phco}(\omega, \lambda, z) - V_{ph}(\omega, \lambda, z, S_f)}{J_{ph}(\omega, \lambda, z, S_f)} \quad (13)$$

The series resistance as a function of recombination velocity for different values of the wavelength is represented in Figure 6:



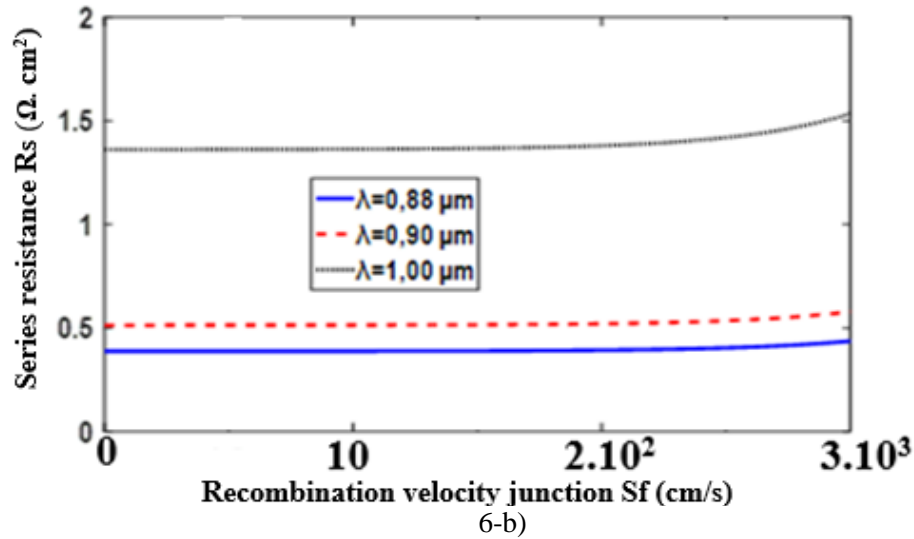


Figure 6: Profile of the series resistance as a function of the recombination velocity at the junction.  
 a) Short wavelength b) Long wavelength  $\omega_r=1.75.10^7$  rad/s;  $z=0.002$  cm

In figures 6-a) and 6-b), we obtain the same calibration curves of the series resistance as a function of the recombination rate at the Sf junction. In figure 6-a) the amplitude of the series resistance decreases when the wavelength increases. A large absorption of the incident photons by the base of the solar cell causes an increased photogeneration of the minority carriers; this results in a low resistivity of the solar cell and consequently a series resistance which decreases. On the other hand, in figure 6-b), the amplitude of the series resistance increases because of a weak absorption of the incident photons by the base, it is as if the solar cell presents a repulsive character of the flow of incident photons, hence a resistivity which becomes high.

**The Shunt Resistance (Rsh)**

To determine the shunt resistance of the photocell, we use the current-voltage characteristics of the figure. This part of the curve corresponds to the short-circuit situation. Under these circumstances, the characteristics of the solar cell are similar to a short-circuit current generator in parallel with the shunt resistor and a load resistor [31]. The equivalent electrical circuit of the photocell operating in a short-circuit situation is shown in Figure 7:

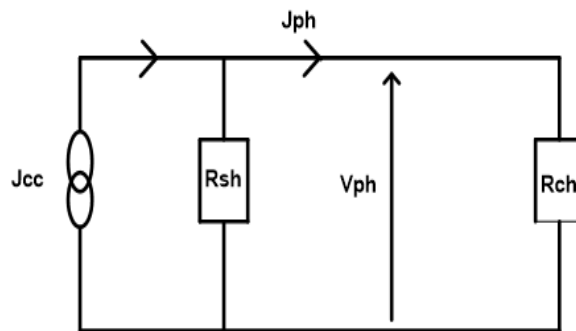


Figure 7: Equivalent electrical circuit of the solar cell operating in a short-circuit situation

By applying the law of meshes to this circuit, we determine the shunt resistance [1, 12]:

$$V_{ph(\omega,\lambda,z,Sf)} = R_{sh(\omega,\lambda,z,Sf)} \times (J_{phcc(\omega,\lambda,z)} - J_{ph(\omega,\lambda,z,Sf)}) \quad (14)$$

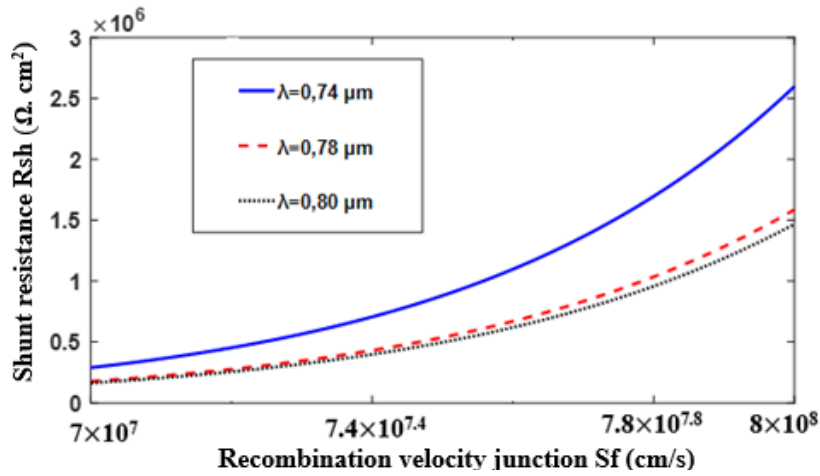


We have the shunt resistance given as follows:

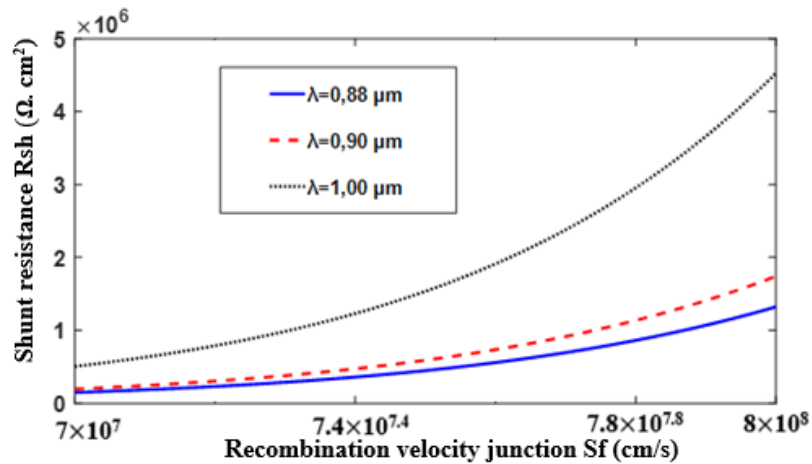
$$R_{sh}(\omega, \lambda, z, S_f) = \frac{V_{ph}(\omega, \lambda, z, S_f)}{J_{phcc}(\omega, \lambda, z) - J_{ph}(\omega, \lambda, z, S_f)} \quad (15)$$

Where  $J_{cc}$  is the short circuit photocurrent density.

The shunt resistance as a function of the recombination velocity at the junction for different values of the wavelength is shown in Figure 8:



8-a)



8-b)

Figure 8: Profile of the shunt resistance as a function of the recombination velocity at the junction. a) Short wavelength b) Short wavelength  
 $\omega_r = 1,75 \cdot 10^7$  rad/s;  $z = 0,002$  cm

In figures 8-a) and 8-b) the calibration curves of the shunt resistance as a function of the recombination velocity at the junction, show the same gaits. For a given curve, the shunt resistance increases with the recombination velocity junction  $S_f$ . For figure, 8-a) the shunt resistance decreases when the wavelength increases: we note that the leakage photocurrent increases and this presages possible recombination of the photogenerated minority carriers at the surfaces. On the other hand in figure 8-b), the shunt resistance increases with the wavelength. It is as if there is an important photogeneration of the non-recombined minority carriers which have a certain kinetic energy to cross the junction.

In table 1 we give some values of series and shunt resistances, for a given value of the magnetic field and angular frequency.

Table 1: Values of  $R_{scomax}$  ( $\Omega.m2$ ) and  $R_{shccmax}$  ( $\Omega.m2$ ) for different wavelength,  $\omega r=1.75.10^6$  rad/s

$\lambda$ ( $\mu m$ )	Gamme des courtes longueurs d'onde			Gamme des grandes longueurs d'onde		
	0,74	0,78	0,80	0,88	0,90	1,00
$Sf=3. 10^3$ cm/s $R_{scomax}$	0,87	0,52	0,48	0,43	0,58	1,53
$Sf=8. 10^8$ cm/s $R_{shccmax}$	$2,63.10^6$	$1,47.10^6$	$1,46. 10^6$	$1,32. 10^6$	$1,72. 10^6$	$4,55. 10^6$

( $R_{scomax}$ ) and ( $R_{shccmax}$ ) are respectively the series resistance in maximum open circuit condition and the shunt resistance in maximum short circuit condition. The parasitic resistances change according to the range of wavelengths considered. A decrease of ( $R_{smax}$ ) and ( $R_{shmax}$ ) with the wavelength in the case of short wavelengths and the opposite effect is observed with long wavelengths.

**Conclusion**

In this work, we have studied the influence of the illumination wavelength on the series and shunt resistance of a polycrystalline silicon solar cell with a vertical series junction under a constant magnetic field, in frequency modulation. The carrier density and the current-voltage characteristic were then determined, and the series and shunt resistances as a function of the recombination rate at the junction for different wavelengths, under a magnetic field, were calculated and theoretically studied. The contribution of the emitter is neglected. For short wavelengths, as the wavelength increases, the series and shunt resistances decrease. For long wavelengths, as the wavelength increases, the shunt and series resistances increase. With the range of short wavelengths, we have more generations of carriers, thus promoting the phenomenon of diffusion. It is the opposite phenomenon for long wavelengths. Therefore, a study of the scattering capacity under the influence of these same parameters is possible.

**References**

- [1]. Diallo, H. L., Dieng, B., Ly, I., Dione, M. M., Ndiaye, M., Lemrabott, O. H., & Sissoko, G. (2012). Determination of the recombination and electrical parameters of a vertical multijunction silicon solar cell. *Research Journal of Applied Sciences, Engineering and Technology*, 4(16), 2626-2631.
- [2]. Van Dyk, E. E., & Meyer, E. L. (2004). Analysis of the effect of parasitic resistances on the performance of photovoltaic modules. *Renewable energy*, 29(3), 333-344. 29(3) pp.333–344.
- [3]. El- Adawi, M.K. and I.A. Al-Nuaim,(2001), “A method to determine the solar cell series resistance from a single I-V characteristic curve considering its shunt resistance-new approach”, *Vacuum*, 64 (1) pp.33-36
- [4]. K. Bouzidi, M. Chegaar and A. Bouhemadou, (2007), “Solar cells parameters evaluation considering the series and shunt resistance”, *Solar Energ. Mater. Solar Cells*, 91(18) pp.1647-1651

- [5]. Wolf, M., & Rauschenbach, H. (1963). Series resistance effects on solar cell measurements. *Advanced Energy Conversion*, 3(2), 455-479.
- [6]. Sharma, A. K., Agarwal, S. K., & Singh, S. N. (2007). Determination of front surface recombination velocity of silicon solar cells using the short-wavelength spectral response. *Solar Energy Materials and Solar Cells*, 91(15-16), 1515–1520.  
<https://doi.org/10.1016/j.solmat.2007.04.018>
- [7]. Mohammad, S. N. (1987). An alternative method for the performance analysis of silicon solar cells. *Journal of Applied Physics*, 61(2), 767–772. <https://doi.org/10.1063/1.338230>
- [8]. Yadav, P., Pandey, K., Tripathi, B., Kumar, C. M., Srivastava, S. K., Singh, P. K., & Kumar, M. (2015). An effective way to analyse the performance limiting parameters of poly-crystalline silicon solar cell fabricated in the production line. *Solar Energy*, 122, 1–10.  
<https://doi.org/10.1016/j.solener.2015.08.005>
- [9]. Green, M.A. (1995). *Silicon Solar Cells Advanced Principles & Practice*. Printed by Bridge Printer Pty. Ltd. 29-35. Dunning Avenue, Roseberry, Centre for Photovoltaic Devices and Systems
- [10]. Ly, I., Ndiaye, M., Wade, M., Thiam, N., Gueye, S., & Sissoko, G. (2013). Concept of Recombination Velocity  $S_{fc}$  at the Junction of a Bifacial Silicon Solar Cell. Steady State, Initiating the Short-Circuit Condition. *Research Journal of Applied Sciences, Engineering and Technology*, 5, 203-208.
- [11]. S. Mbodji, I. Ly, H. L. Diallo, M.M. Dione, O. Diassé and G. Sissoko(2012), “Modeling Study of N+/P Solar Cell Resistances from Single I-V Characteristic Curve Considering the Junction Recombination Velocity ( $S_f$ )” *Research Journal of Applied Sciences, Engineering and Technology* 4(1) pp.1-7
- [12]. Sy, K.M., Diene, A., Tamba, S., Diouf, M.S., Diatta, I., Dieye, M., Traore, Y., & Sissoko, G. (2016), “Effect of temperature on transient decay induced by charge removal of a silicon solar cell under constant illumination”, *Journal of Scientific and Engineering Research*, 3(6)pp. 433-445
- [13]. Zondervan, A., Verhoef, L. A., & Lindholm, F. A. (1988), “Measurement circuits for silicon-diode and solar-cell lifetime and surface recombination velocity by electrical short-circuit current decay”, *IEEE Transactions on Electron Devices*, 35(1) pp.85–88
- [14]. Sahin, G., Dieng, M., El Moujtaba, M. A. O., Ngom, M. I., Thiam, A., & Sissoko, G.,(2015), “Capacitance of Vertical Parallel Junction Silicon Solar Cell under Monochromatic Modulated Illumination”, *Journal of Applied Mathematics and Physics*, 3(11) pp.1536-1543.  
<http://dx.doi.org/10.4236/jamp.2015.311178>
- [15]. Ba, F., Seibou, B., Wade, M., Diouf, M.S., Ly, B., & Sissoko, G., (2016), “Equivalent Electric Model of the Junction Recombination Velocity limiting the Open Circuit of a Vertical Parallel Junction Solar Cell under Frequency Modulation”. *IPASJ International Journal of Electronics & Communication*,4(7)pp. 1-11.
- [16]. J. H. Scofield, (1995), “Effects of series resistance and inductance on solar cell admittance measurements”, *Solar Energy Materials and Solar Cells*, 37 (2) pp.217-233
- [17]. Pozner, R., Segev, G., Sarfaty, R., Kribus, A., & Rosenwaks, Y.(2011), “Vertical junction Si cells for concentrating photovoltaics. Progress in Photovoltaics”, *Research and Applications*, 20(2)pp. 197–208.
- [18]. F. Agyenim, N. Hewitt, P. Eames, and M. Smyth, (2010), “A review of materials, heat transfer and phase change problem formulation for latent heat thermal energy storage systems (LHTESS),” *Renewable Sustainable Energy Rev.*, vol. 14(2) pp.615-628
- [19]. J D Mondol, M Smyth, A Zacharopoulos, and T Hyde, (2009), “Experimental performance evaluation of a novel heat exchanger for a solar hot water storage system,” *Appl. Energy*, 86(9) pp. 1492-1505

- 
- [20]. Amadou Diao, N. Thiam, M. Zoungrana, G.Sahin, M Ndiaye, G Sissoko, (2014), “Diffusion Coefficient in Silicon Solar Cell with Applied Magnetic Field and under frequency: Electric Equivalent Circuits”, *World Journal of Condensed Matter Physics*, 4(2) pp.84-92
- [21]. J.N. Hollenhorst, and G. Hasnain, (1995), “Frequency dependent hole diffusion in InGaAs double heterostructures”, *Appl. Phys. Lett*, 67 (15) pp.2203 – 2205.
- [22]. Th. Flohr and R. Helbig, (1989) “Determination of minority-carrier lifetime and surface recombination velocity by Optical-Beam-Induced-Current measurements at different light wavelengths” *J. Appl. Phys.* Vol.66 (7), pp 3060 – 3065.
- [23]. Th. Flohr and R. Helbig. (1989) “Determination of minority-carrier lifetime and surface recombination velocity by Optical-Beam-Induced-Current measurements at different light wavelengths” *J. Appl. Phys.* Vol.66 (7), pp 3060 – 3065.
- [24]. Thiam, N., Diao, A., Ndiaye, M., Dieng, A., Thiam, A., Sarr, M., Maiga, A. S., Sissoko, G., (2012), “Electric Equivalent Models of Intrinsic Recombination Velocities of a Bifacial Silicon Solar Cell under Frequency Modulation and Magnetic Field Effect” *Research Journal of Applied Sciences, Engineering and Technology* 4(22) pp.4646-4655
- [25]. G. Sissoko, S. Sivoththanam, M. Rodot, P. Mialhe (1992). Constant illumination-induced open circuit voltage decay (CIOCVD) method, as applied to high efficiency Si Solar cells for bulk and back surface characterization. *11th European Photovoltaic Solar Energy Conference and Exhibition*, poster 1B, Montreux, Switzerland., pp.352-354
- [26]. H. L. Diallo, A. Seïdou Maiga, A. Wereme and G. Sissoko, (2008). New approach of both junction and back surface recombination velocities in a 3D modelling study of a polycrystalline silicon solar cell. *Eur. Phys. J. Appl. Phys.*, 42(03) pp. 203-211
- [27]. Fossum, J. G., (1977), “Physical operation of back-surface-field silicon solar cells”, *IEEE Transactions on Electron Devices*, 24(04) pp. 322–325
- [28]. Mountaga Boiro, Babou Dione, Ibrahima Toure, Adama Ndiaye, Amadou Diao. (2022). Influence of the Magnetic Field on the Diffusion Capacitance of a Serial Vertical Junction Silicon Solar Cell in Frequency Modulation. *American Journal of Modern Physics*. Vol. 11(1) pp. 1-6. doi: 10.11648/j.ajmp.20221101.11
- [29]. S. Mbodj, I. Ly, A. Dioume, H. L. Diallo, I.F. Barro, G. Sissoko, (2006). Equivalent electric circuit of a bifacial solar cell in transient state under magnetic field, *21st European Photovoltaic Solar Energy Conference, Dresden, Germany*, pp.447-450.
- [30]. Gregoire Sissoko, C. Museruka, A. Correa, I. Gaye and A.L. Ndiaye, (1996). Light Spectral Effect on Recombination Parameters of Silicon Solar Cell, *The 4th Proceedings of the World Renewable Energy Congress, Denver, USA*, Part III, 15-21. pp.1487 - 1490.
- [31]. M. Bashahu, A. Habyarimana (1995). Review and test of methods for determination of the solar cell series resistance. *Renewable Energy*, 6 (2) pp. 127-138
- [32]. D. Pysch, A. Mette, S.W. Glunz (2007). A review and comparison of different methods to determine the series resistance of solar cells. *Sol Energy Mater Sol Cells*, 91(18) pp. 1698-1706
-